Toward self-powered and reliable visible light communication using amorphous silicon thin-film solar cells

MEIWEI KONG,[1,3] JIAMING LIN,[2,3] CHUN HONG KANG,[1] CHAO SHEN,[1] YUJIAN GUO,[1] XIAOBIN SUN,[1] MOHAMMED SAIT,[1] YANG WENG,[1] HUAFAN ZHANG,[1] TIEN KHEE NG,[1] AND BOON S. OOI[1,*]

[1] *Photonics Laboratory, King Abdullah University of Science and Technology (KAUST), Thuwal 21534, Saudi Arabia*
[2] *Optical Communications Laboratory, Ocean College, Zhejiang University, Zheda Road 1, Zhoushan, Zhejiang, 316021, China*
[3] *Both Authors Contributed Equally*
**boon.ooi@kaust.edu.sa*

Abstract: Enhancing robustness and energy efficiency is critical in visible light communication (VLC) to support large-scale data traffic and connectivity of smart devices in the era of fifth-generation networks. To this end, we demonstrate that amorphous silicon (a-Si) thin-film solar cells with a high light absorption coefficient are particularly useful for simultaneous robust signal detection and efficient energy harvesting under the condition of weak light in this study. Moreover, a first-generation prototype called AquaE-lite is developed that consists of an a-Si thin-film solar panel and receiver circuits, which can detect weak light as low as 1 μW/cm^2. Using AquaE-lite and a white-light laser, orthogonal frequency-division multiplexing signals with data rates of 1 Mb/s and 908.2 kb/s are achieved over a 20-m long-distance air channel and 2.4-m turbid outdoor pool water, respectively, under the condition of strong background light. The reliable VLC system based on energy-efficient a-Si thin-film solar cells opens a new pathway for future satellite-air-ground-ocean optical wireless communication to realize connectivity among millions of Internet of Things devices.

1. Introduction

The race to develop fifth-generation (5G) networks has begun worldwide. Compared with fourth-generation (4G) networks, multiple design objectives are defined for 5G networks, such as targeting data rates as high as 10 Gb/s, reducing power consumption by nearly 90%, improving network availability and reliability, and supporting massive connectivity of Internet of Things (IoT) devices [1]. To fulfill data traffic requirements, visible light communication (VLC) technology, which offers ~1,200 times the bandwidth of the congested radio-frequency spectrum of 300 GHz, is envisioned to be a major enabler [2, 3]. Moreover, it is expected to support large-scale deployments of low-power consuming devices by employing existing energy-efficient lighting infrastructures (i.e., light emitting diodes (LEDs)) as light sources for simultaneous illumination and high-speed wireless data transmission [3]. Driven by the rapid escalation of energy-saving requirements, solar cells with the dual functions of energy harvesting and data acquisition are appealing as alternatives to commonly used detectors (i.e., positive-intrinsic-negative diodes and avalanche photodiodes) [3–11]. They are widely recognized as the key components of future self-powered IoT devices such as wearables, smart homes, smart transportation systems, and long-term environmental monitoring equipment with millions of sensors [3]. However, the energy-efficient VLC technologies based on LEDs and solar cells are still in their infancy [4–8]. As most related works have focused on improving data rates (~Mb/s), transmission distances are still limited to ~cm, which ascribes to the low

power density of LEDs and the low absorption coefficient of the used crystalline silicon (Si) solar cells [4–7]. Considerable effort is still required to support high-availability, high-reliability, and cost-effective heterogeneous data traffic in future 5G networks.

Amorphous silicon (a-Si) thin-film solar cells would be particularly useful for implementing reliable and energy-efficient VLC. The first reason for this is that the light absorption coefficient of a-Si thin-film solar cells is much higher than that of crystalline Si in the visible light spectrum due to the presence of band tail states, which allows a-Si thin-film solar cells to have a higher response to weak visible light [12, 13]. Second, a-Si thin-film solar cells are translucent and can be deposited on various flexible substrates for mass production with low cost, which facilitates the future integration of a-Si thin-film solar cells into a wide range of IoT devices. In this study, to implement simultaneous reliable VLC and efficient energy harvesting, a first-generation prototype called AquaE-lite is developed that consists of an a-Si thin-film solar panel with a large detection area of 144 cm^2 and receiver circuits with a total power consumption of only 370 mW. AquaE-lite can detect weak light as low as 1 $\mu W/cm^2$ and thus allows for a highly robust system even when tested under challenging conditions such as an outdoor pool with turbid water and direct sunlight. This suggests that a-Si thin-film solar cells can serve most effectively as tools for simultaneous weak-light signal detection and efficient energy harvesting in power-shortage marine environments. Employing a white-light laser, we achieve a 20-m long-distance illumination and VLC with a data rate of 1 Mb/s in the air. Compared with organic, polycrystalline Si, or monocrystalline Si solar cells employed in the prior work [3–9], a-Si thin-film solar cells with the superiority in weak-light detection show excellent performance in long-distance VLC. White-light lasers are also proved to be good candidates of white-light LEDs to implement simultaneous long-distance lighting and high-speed VLC in the future thanks to their better collimation, higher bandwidth and higher power intensity. Moreover, compared with red/blue-light lasers as light sources in [3] and [9], the use of white-light lasers is favorable in increasing the energy conversion efficiency of the solar cells. The most exciting application scenario we envisage is power-hungry satellites, unmanned aerial vehicles (UAV), buoys, and various underwater vehicles and sensors that integrate a-Si thin-film solar cells for long-term self-power satellite-air-ground-ocean (SAGO) optical wireless communication, which will considerably accelerate the pace of realizing global IoT.

2. Experimental setup

Figure 1(a) shows the experimental setup of the AquaE-lite and white-light laser-based VLC system. Orthogonal frequency-division multiplexing (OFDM) technology with high spectral efficiency was employed in the experiment. 4-QAM OFDM signals were generated offline by MATLAB and uploaded to an arbitrary waveform generator (AWG, Tektronix AWG70002A). The main parameters of the VLC system using OFDM are listed in Table 1. After being transmitted through a 25-dB amplifier (AMP, Mini-Circuits ZHL-6A+) and a key-press variable electrical attenuator (ATT, KT2.5-60/1S-2S), output signals were superposed onto a white-light laser (SaNoor Technologies, SNWL-3A) using a bias-Tee (Bias-T, Tektronix PSPL5580). The bias current of the white-light laser was set to 570 mA in the experiment. The AMP was used to amplify the OFDM signals, and the ATT was used to adjust the amplitudes of the OFDM signals within the linear operation range of the white-light laser. Propagating through air channels with different distances, the directly modulated optical signals were detected by AquaE-lite. Finally, the output signals were captured by a mixed signal oscilloscope (MSO, Tektronix DPO 72004C) and demodulated offline. Figure 1(b) is the experimental scene diagram. As the experiment was conducted during the day time, sunlight entering through a window and indoor fluorescent lights were the main background noise. At the receiver side, AquaE-lite consists of an a-Si thin-film solar panel and receiver circuits. Four off-the-shelf a-Si thin-film solar cells were connected in series and thus provided a total active area of 144 cm^2 (12 × 12 cm), as shown in Fig. 1(c). In each of the a-Si thin-film solar cells, four individual sub-cells were connected in parallel. To achieve the balance of energy budget, an a-Si thin-film

solar cell in the lower left corner of the whole solar panel with a length of 6 cm and width of 6 cm was used for simultaneous VLC and energy harvesting, while the other three a-Si thin-film solar cells were primarily used for energy harvesting in circuit design.

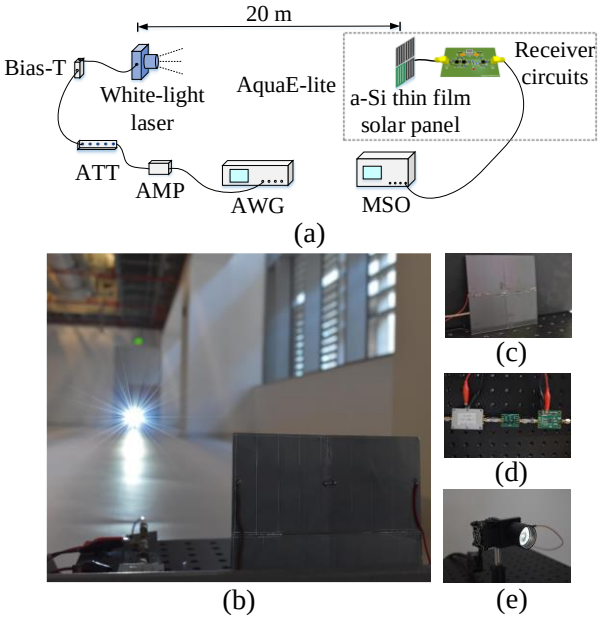

Fig. 1. (a) Experimental setup of the white-light laser and a-Si thin-film solar panel-based VLC syste, (b) experimental scene, (c) a-Si thin-film solar panel, (d) receiver circuits, and (e) white-light laser.

Table 1. Main parameters of the VLC system using OFDM

Parameters	Values		
Data rate of OFDM signals	1.2 Mb/s	1 Mb/s	908.2 kb/s
Number of subcarriers	123	103	93
Bit number of pseudorandom binary sequence	2^{20}-1		
Inverse fast Fourier transform size	1024		
Number of cyclic prefix	10		
Number of subcarriers for frequency gap near DC	10		
Number of OFDM symbols (including two training symbols for timing synchronization and four training symbols for channel equalization)	154		
Sampling rate of AWG	5 MSamples/s		
Sampling rate of MSO	25 MSamples/s		

The receiver circuits were composed of a signal processing (SP) module, a band-pass filter (BPF), and a low noise amplifier (LNA), as shown in Fig. 1(d). In the SP module, AC signals were separated and then processed to overcome the problem of signal attenuation and deformation at the receiver side. The BPF with a bandwidth of 0 to 2 MHz was employed to remove the background noise. The LNA with a bandwidth of 0 to 2 MHz was used to amplify the amplitudes of the received signals and thus improve the signal-to-noise ratio at the receiver. The total electrical power consumption of the receiver circuits was only 370 mW by using these low-power components. The high-speed white-light laser as shown in Fig. 1(e) consists of a blue GaN laser diode and ceramic phosphor plate. A heat sink, a thermoelectric cooler (TEC) module, and a thermistor were also integrated into it. A laser diode and TEC driver (SaNoor Technologies, SNLC-1A-TEC) was used to control the temperature of the white-light laser. A

plano-convex lens mounted in front of the white-light laser was used to change the focal length and thus implement lighting as well as communication at different distances.

3. Experimental results

Figure 2(a) illustrates the current density versus voltage (*J-V*) curve of an a-Si thin-film solar cell in the dark and under an illumination intensity of 100 mW/cm^2 using an air mass 1.5 global (AM 1.5 G) solar simulator (Asashi Spectra, HAL-320). From the curve, we determined that the a-Si thin-film solar cell had an open-circuit voltage (V_{oc}) of 3.33 V, a short-circuit current density (J_{sc}) of 2.27 mA/cm2, a fill factor (*FF*) of 62.97%, and a solar power conversion efficiency (*PCE*) of 4.80%. Thus, the maximum solar power (P_{max}) harvested by an a-Si thin-film solar cell is approximately 171.76 mW. By using the AquaE-lite system consisted of four solar cells, we inferred that the energy harvested is more than sufficient to power the receiver circuits for VLC, as the total electrical power consumption of the receiver circuits was only 370 mW. To demonstrate the capability of the a-Si thin-film solar cell in weak light detection, we measured the current density of the a-Si thin-film solar cell under different power intensities. A solar simulator was used as the light source for the measurement. A one-sun calibrated detector (Asashi Spectra, CS-0) was used to monitor the power intensity of the solar spectrum and thus ensure uniformity of irradiance. As shown in Fig. 2(b), the measured current density of the a-Si thin-film solar cell was reduced with respect to the decrement of the power density. At the lowest possible illumination of 10^{-1} mW/cm^2, the a-Si thin-film solar cell still exhibited a high current density of 2.6 μA/cm^2 because of its sufficiently low dark current density of approximately 3.2 nA/cm^2, thus ensuring a sufficiently large separation between the dark and light currents for weak light detection. Due to the low dark current exhibited by the a-Si thin-film solar cell and assuming a good linear dynamic response, we anticipated that the device is capable of weak light detection of 1 μW/cm^2. A similar report on the high feasibility of a-Si thin-film solar cells for weak light detection was also previously reported by Schubert et al. [12].

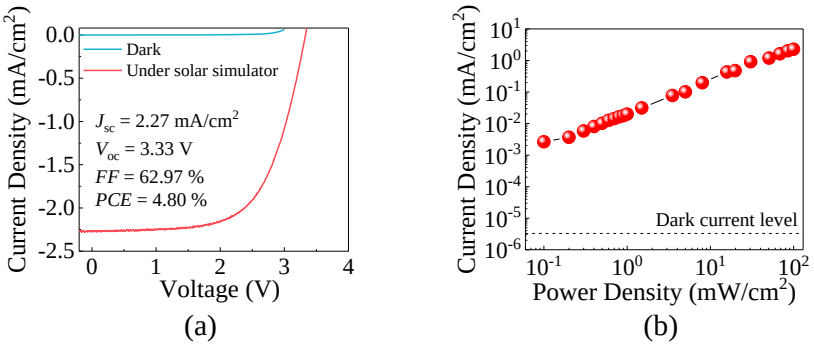

Fig. 2. (a) *J-V* curve of an a-Si thin-film solar cell in the dark and under an illumination intensity of 100 mW/cm^2 using the AM 1.5 G solar simulator, and (b) current densities of the a-Si thin-film solar cell under different power densities.

Figure 3(a) presents light-current-voltage (*L-I-V*) characteristics of the white-light laser at 25°C, which show good linearity. The threshold current and threshold voltage were approximately 380 mA and 3.5 V, respectively. The optical spectrum of the white-light laser under the drive current of 570 mA is shown in Fig. 3(b). The peak wavelength was 448 nm. Figure 3(c) shows the Commission Internationale de l'Eclairage (CIE) 1931 diagram with chromaticity coordinates (x, y) of the white-light laser. It exhibited CIE coordinates, a correlated color temperature (CCT) value, and color rendering index (CRI) of (0.3253, 0.3637), 5788 K, and 62.3, respectively. The beam shape and power distribution of the white-light laser measured with a beam profiler are shown in Fig. 3(d), which presents a Gaussian distribution. The figure shows that the approximate circle has a radius of 2.5 mm. After being transmitted

through air channels with different distances, the light formed light spots of different sizes at the receiving end. As the beam shape still presented a Gaussian distribution, we measured eight points of illuminances along the x axis and then extended the beam in all directions to obtain the illuminance distribution at the receiving plane.

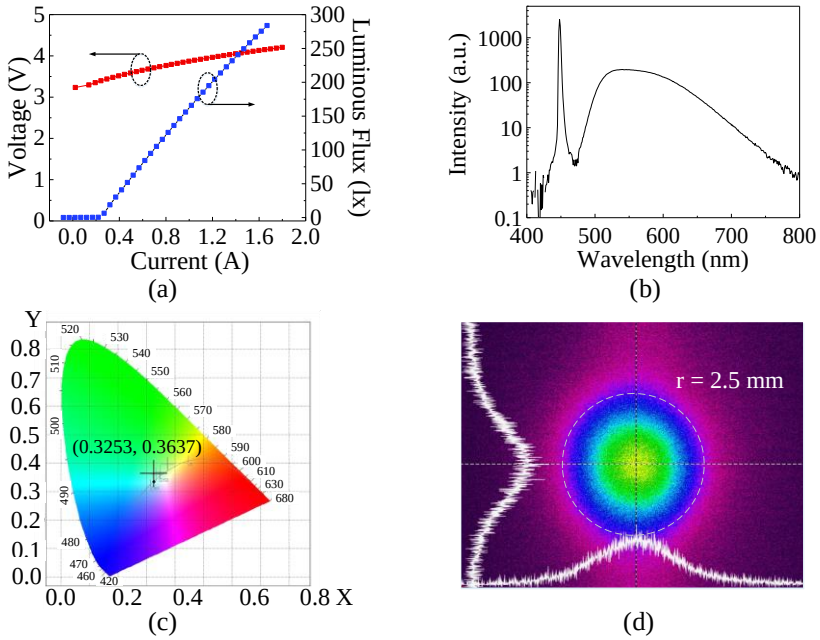

Fig. 3. (a) *L-I-V* characteristics of the white-light laser, (b) optical spectrum of the white-light laser under a drive current of 570 mA, (c) CIE 1931 diagram with chromaticity coordinates (x, y) of the white-light laser, and (d) beam shape and power distribution of the white-light laser.

Figure 4 depicts the illuminance distributions within an area of 1385 cm^2 at distances of 5, 10, 15, and 20 m. Average illuminances on the a-Si thin-film solar cell used for communication at distances of 10, 15, and 20 m were 286.93, 109.54, and 79.95 lx, respectively. In the experiment, a light spot with an area of ~2922 cm^2 (diameter: 61 cm) could be observed at a distance of 20 m, which was much larger than that of the a-Si thin-film solar panel (144 cm^2). This large light spot not only can be used for long-distance illumination, but also can significantly reduce the requirements on link alignment. Moreover, the average irradiance on the a-Si thin-film solar cell at a distance of 5 m was only approximately 0.2 mW/cm^2, which was measured by the one-sun calibrated detector. Note that because of the limitation of the measuring range of the one-sun calibrated detector (0.1 mW/cm^2 - 1 W/cm^2), the average irradiances of the white-light laser at distances of 10, 15, and 20 m could not be accurately determined. However, we inferred that they were much less than 0.2 mW/cm^2. Based on this limited average irradiance, we studied the performances of both the white-light laser and the a-Si thin-film solar-cells-based VLC system.

First, we measured the frequency response of the whole system at a transmission distance of 20 m. The 3-dB bandwidth of the system was not greater than 290 kHz, as shown in Fig. 5(a), which was limited by the bandwidth of the a-Si thin-film solar panel. We then assessed the superiority of the white-light laser and AquaE-lite in implementing long-distance VLC using OFDM. Figure 5(b) illustrates bit error rates (BERs) of the 908.2-kb/s, 1-Mb/s, and 1.2-Mb/s 4-QAM OFDM signals at transmission distances of 10, 15, and 20 m. Over a 15-m air channel (with average illuminance of 109.54 lx), the data rate could achieve 1.2 Mb/s with a BER of 3.713×10^{-3}, which was below the forward error correction (FEC) limit of 3.8×10^{-3}. A data rate of 1-Mb/s OFDM signals with a BER of 1.642×10^{-3} could be achieved after

transmission through a 20-m air channel (with average illuminance of 79.95 lx). It proved that the illuminance of the white-light laser can significantly affect the performance of the a-Si thin-film solar panel-based communication system and AquaE-lite has very good performance in detecting weak-light signals. Moreover, according to Fig. 4, we inferred that the data rate of 1 Mb/s could still be achieved in the illumination areas with radiuses of around 15 cm, 24 cm, 18 cm, and 9 cm at the distances of 5 m, 10 m, 15 m, and 20 m, respectively. It means that the AquaE-lite and white-light laser-based VLC system has great potential to resolve link alignment issues.

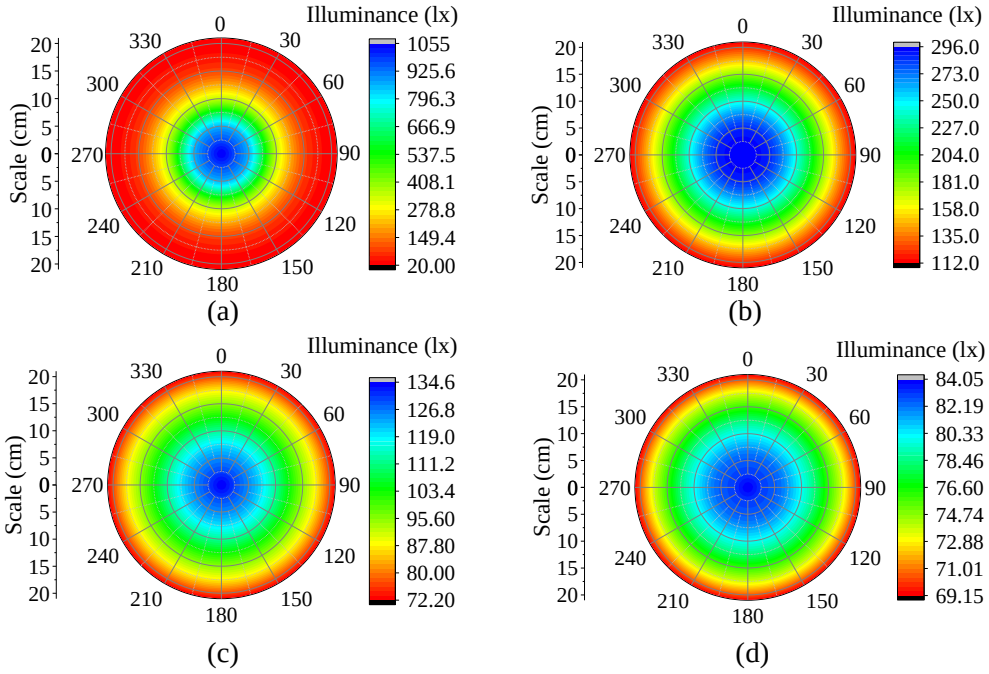

Fig. 4. Illuminance distributions at distances of (a) 5 m, (b) 10 m, (c) 15 m, and (d) 20 m.

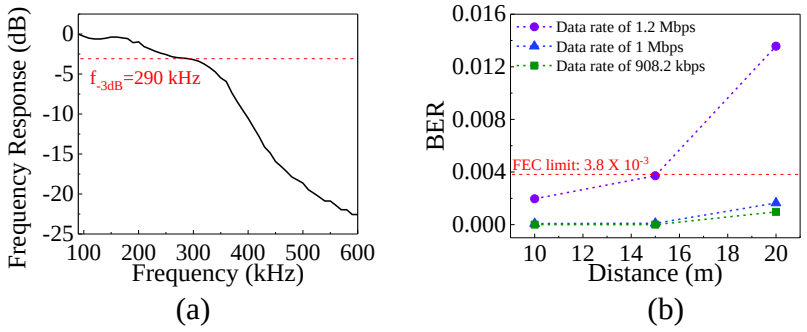

Fig. 5. (a) Frequency response of the whole system measured at a transmission distance of 20 m, and (b) BERs of 908.2-kb/s, 1-Mb/s, and 1.2-Mb/s 4-QAM OFDM signals at transmission distances of 10, 15, and 20 m.

4. Field trials

To investigate the energy harvesting performance of Aqua-E-lite, we conducted a field test under the bright sunlight (~40 mW/cm^2) at 11:00 AM on 16th Oct, 2019 in King Abdullah University of Science and Technology, Saudi Arabia. Figure 6 presents the experimental scene. An optical spectrometer (GL SPECTIS 5.0 VIS) was employed to measure the solar spectrum. The one-sun calibrated detector was used to measure the illumination intensity of sunlight.

Firstly, we measured the *J-V* curve of one single a-Si thin-film solar cell under the sun. As shown in Fig. 7(a), the maximum solar power generated by the a-Si thin-film solar cell is 126 mW. Then, under the same circumstances, we connected three a-Si thin-film solar cells in series for energy harvesting to measure the maximum generated power. From the *J-V* curve of the three a-Si thin-film solar cells connected in series (Fig. 7(b)), we calculated that their maximum generated power was 474 mW, which was more than three times that generated by one a-Si thin-film solar cell (126 mW). As four a-Si thin-film solar cells connected in series were used for energy harvesting in AquaE-lite, we inferred that their maximum generated power would be high enough to power the receiver circuit which consumed power of 370 mW. In the future, by adding a power management module with wake-up strategies, a fully energy-autonomous solar cell receiver would be implemented.

Fig. 6. Experimental scene.

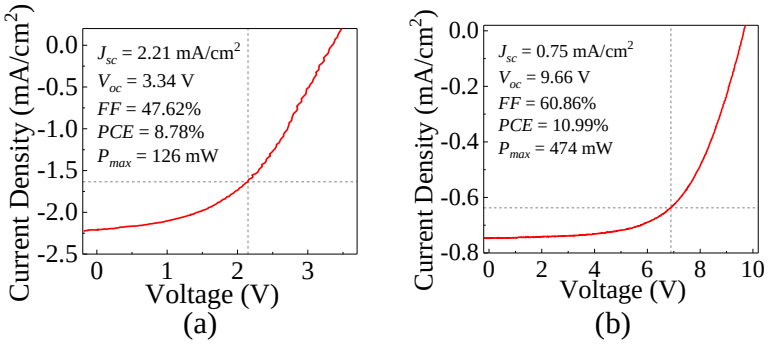

Fig. 7. Under an illumination intensity of 40 mW/cm^2, (a) *J-V* curve of one single a-Si thin-film solar cell and (b) *J-V* curve of three a-Si thin-film solar cells connected in series.

We further demonstrated the weak-light detection performance of AquaE-lite in a more challenging setting, namely, an outdoor pool under the condition of direct sunlight. The absorption coefficient of the pool water was 0.01 m^{-1}. The scattering coefficient of the pool water was 0.36 m^{-1}, which approximated that of coastal water. Figure 8(a) shows the experimental scene. The white-light laser and AquaE-lite were separately installed in two capsules and placed at the bottom of the pool, as shown in Figs. 8(b) and 8(c). Other equipment and components at the transmitting and receiving ends were placed on the shore, which were the same as those in Fig. 1(a). A remotely operated vehicle (ROV) was employed to monitor the underwater environment in real time.

In the experiment, the white-light laser beam was perpendicular to the surface of the a-Si thin-film solar panel. The 908.2-kb/s 4-QAM OFDM signals were transmitted at different distances. At a distance of 2.4 m, the measured BER was 1.010×10^{-3}, which was below the FEC limit. Figure 9 shows BERs of the received OFDM signals for different subcarriers. Higher BERs in the low-frequency region were caused by background noise. Higher BERs in the high-

frequency region were due to the limited bandwidth of the a-Si thin-film solar panel. The inset shows the corresponding constellation map, which is well converged and indicates the robustness of a-Si thin-film solar cells in detecting weak light under the condition of strong background light. In addition, a-Si thin-film solar cells with the advantages of being translucent and flexible and having a high absorption coefficient and low cost present great prospects for future self-powered Internet of Underwater Things devices, which can greatly alleviate underwater energy-shortage issues.

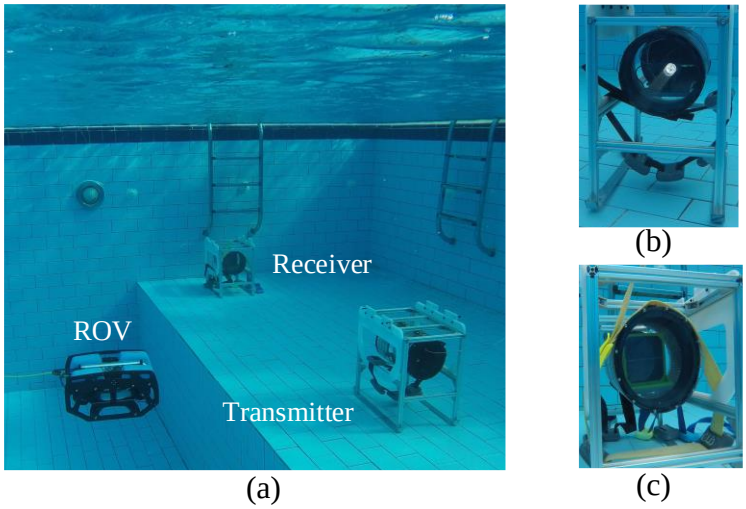

Fig. 8. (a) Experimental scene, (b) transmitter: white-light laser, and (c) receiver: AquaE-lite.

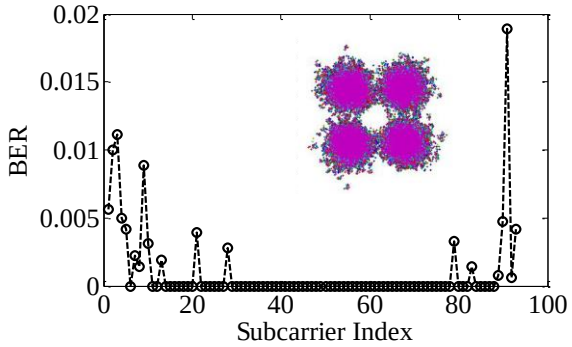

Fig. 9. BERs of the received OFDM signals for different subcarriers over 2.4-m outdoor pool water. Inset: the corresponding constellation map.

5. Conclusions

In conclusion, a-Si thin-film solar cells and white-light lasers have great potential in future practical VLC applications such as long-distance VLC in the air and more challenging underwater VLC. The developed prototype called AquaE-lite consisting of a-Si thin-film solar cells and receiver circuits could support weak light detection of 1 μW/cm^2. Over a 15-m air channel, the average illuminance on the a-Si thin-film solar panel was 109.54 lx and the corresponding achieved data rate of OFDM signals was 1.2 Mb/s. Over a 20-m air channel, the area of the light sport increased to ~2922 cm^2 and the average illuminances on the a-Si thin-film solar panel decreased to 79.95 lx. In these circumstances, 1-Mb/s OFDM signals could still be successfully transmitted with only a 290-kHz modulation bandwidth of the a-Si thin-film solar panel. This verified the feasibility of the white-light laser and a-Si thin-film solar-

cells-based long-distance lighting and VLC. We also inferred the offset tolerances at different transmission distances, which indicates that the proposed system has great potential in alleviating link alignment issues. Furthermore, over 2.4-m turbid outdoor pool water with direct sunlight, 908.2-kb/s OFDM signals were achieved, which demonstrated the robustness of the a-Si thin-film solar-cells-based VLC system. Further development and application of this technology is underway. As power balance was achieved by AquaE-lite under the bright sunlight, the second-generation AquaE-lite is expected to be fully energy-autonomous with the addition of power management circuits. In the next phase, to implement SAGO communication, AquaE-lite will be integrated with UAVs, buoys, underwater vehicles, and sensors and will then be deployed to the Red Sea for long-term monitoring of underwater environments.

Funding

King Abdullah University of Science and Technology (KAUST) (baseline funding, BAS/1/1614-01-01, KAUST funding KCR/1/2081-01-01, and GEN/1/6607-01-01); King Abdulaziz City for Science and Technology (KACST) Grant KACST TIC R2-FP-008.

References

1. M. Agiwal, A. Roy, and N. Saxena, "Next generation 5G wireless networks: A comprehensive survey," IEEE Commun. Surv. Tutorials **18**(3), 1617–1655 (2016).
2. H. M. Oubei, C. Shen, A. Kammoun, E. Zedini, K. H. Park, X. Sun, G. Liu, C. H. Kang, T. K. Ng, M. S. Alouini, and B. S. Ooi, "Light based underwater wireless communications," Jpn. J. Appl. Phys. **57**(8S2), 08PA06 (2018).
3. S. Zhang, D. Tsonev, S. Videv, S. Ghosh, G. A. Turnbull, I. D. Samuel, and H. Haas, "Organic solar cells as high-speed data detectors for visible light communication," Optica **2**(7), 607–610 (2015).
4. S. M. Kim, J. S. Won, and S. H. Nahm, "Simultaneous reception of solar power and visible light communication using a solar cell," Opt. Eng. **53**(4), 046103 (2014).
5. Z. Wang, D. Tsonev, S. Videv, and H. Haas, "Towards self-powered solar panel receiver for optical wireless communication," in *IEEE International Conference on Communications (ICC)* (IEEE, 2014), pp. 3348–3353.
6. W. H. Shin, S. H. Yang, D. H. Kwon, and S. K. Han, "Self-reverse-biased solar panel optical receiver for simultaneous visible light communication and energy harvesting," Opt. Express **24**(22), A1300–A1305 (2016).
7. B. Malik and X. Zhang, "Solar panel receiver system implementation for visible light communication," in *Proceedings of IEEE International Conference on Electronics, Circuits, and Systems* (IEEE, 2016), pp. 502–503.
8. X. Chen, C. Min, and J. Guo, "Visible light communication system using silicon photocell for energy gathering and data receiving," Int. J. Opt. **2017**, 1–5 (2017).
9. M. Kong, B. Sun, R. Sarwar, J. Shen, Y. Chen, F. Qu, J. Han, J. Chen, H. Qin, and J. Xu, "Underwater wireless optical communication using a lens-free solar panel receiver," Opt. Commun. **426**, 94–98 (2018).
10. Z.Wang, D. Tsonev, S.Videv, and H. Haas, "On the design of a solar-panel receiver for optical wireless communications with simultaneous energy harvesting," IEEE J. Sel. Areas Commun. **33**(8), 1612–1623 (2015).
11. H. Y. Wang, J. T. Wu, C. W. Chow, Y. Liu, C. H. Yeh, X. L. Liao, K. H. Lin, W. L. Wu, and Y. Y. Chen, "Using pre-distorted PAM-4 signal and parallel resistance circuit to enhance the passive solar cell based visible light communication," Opt. Commun. **407**, 245–249 (2018).
12. M. B. Schubert and J. H. Werner, "Flexible solar cells for clothing," Mater. Today **9**(6), 42–50 (2006).
13. K. Gmucová and J. Müllerová, "Amorphous photovoltaics: organics versus inorganics," in *Amorphous Materials*, S. B. Mishra, ed. (Nova Science Publishers Inc, UK, 2013).